Melting and Phase Space Transitions in Small Ionic Clusters

F. Calvo* and P. Labastie

Laboratoire Collisions, Agrégats, Réactivité (UMR 5589, CNRS), IRSAMC, Université Paul Sabatier, 118 Route de Narbonne, 31062 Toulouse Cédex 4, France

Received: November 7, 1997; In Final Form: January 6, 1998

We investigate the thermodynamical behavior of small neutral sodium fluoride clusters using both Monte Carlo (MC) and molecular dynamics (MD) simulations. The three clusters studied, $(NaF)_n$ with $n = 6$, 7, and 13, all display thermodynamical phases of a solidlike nature at low temperature and liquidlike at higher temperatures. However, unlike van der Waals clusters, the melting process appears to be a multistage phenomenon: The clusters undergo successive transitions toward more fully fluid states. We relate this behavior to the isomerization processes occurring in these systems and the topography of the potential energy surface. As one of our indicators, we calculate the largest Liapunov exponent λ as a function of the total energy E. The slope of $\log \lambda(E)$ strongly drops at the onset of first isomerization. The subsequent fluid transitions are not associated with mere changes in this slope. In view of this fact, we conclude that the degree of chaos in the dynamics of the system is not sensitive to the total volume of accessible phase space, once the lowest saddle points are allowed to be crossed.

I. Introduction

The interest in phases and phase transitions in clusters has considerably grown since the seminal works of Briant and Burton[1] and Kaelberer and Etters[2] in the 1970s. For about two decades, many theoretical and numerical studies have focused on weakly bound van der Waals clusters, modeled either by the Lennard−Jones (LJ) 6−12 potential[3] or by the Morse potential.[4] This latter potential takes into account more precisely the range of interaction.[5,6] An interesting feature of the numerical experiments was the discovery of a "dynamical coexistence" range joining the solidlike, rigid phase to the liquidlike, much disordered phase.[7] It was shown by several authors,[8] particularly Berry and Wales,[9] that this phenomenon was indeed a finite size rounding of the first-order solid−liquid transition in the bulk.

While the global thermodynamical behavior of rare gas clusters was becoming fairly well understood, other kinds of clusters began to be studied. Molecular clusters were mostly investigated in the group of Fuchs.[10] These authors found several interesting phenomena peculiar to these systems, such as a solid−solid transition in $(SF_6)_n$ clusters[11] and an orientational phase change in $(N_2)_n$ clusters,[12] the beginning of the bulk solid−plastic transition. Alkali clusters[13] also display phases and phase changes and show a special transition associated with surface melting in Na_{20}.[14] Indeed, the phenomenon of surface melting may be more general in finite size atomic systems, since it has been observed in other clusters.[15−19] More recently, investigations on fullerenes[20] revealed a new "pretzel phase" made of floppy carbon strings, intermediate between the solid and liquid.

Among the large variety of other model clusters studied in the context of phase transitions, alkali halides have been devoted several studies, theoretical as well as experimental.[21−27] In fact, the Born−Mayer potential[21] generally used to describe these ionic clusters is accurate enough to produce good static results in agreement with the structures found by spectroscopy. It is also simple enough to provide satisfactory statistical data.

* Corresponding author. E-mail: florent@yosemite.ups-tlse.fr.

As first noted by Luo et al.,[22] these systems offer very different thermal behaviors, depending on the cluster size and structure. The simple isomerization processes in the $(NaCl)_4$ cluster were observed to become a sharp melting transition in $(NaCl)_{108}$, whereas $(NaCl)_{16}$ has features shared by both the smaller and larger sizes. Subsequent studies[23−25] emphasized the importance of isomerization in alkali halide clusters. In particular, Rose and Berry[25] investigated the melting of $(KCl)_n$, $n = 4$ and 5, using molecular dynamics (MD) simulations. They found the dynamical coexistence between solidlike and disordered phases, especially in the "magic" $2 \times 2 \times 2$ cluster, K_4Cl_4. The next magic size, $(KCl)_{32}$, was also studied by the same authors.[26,27] Besides clear evidence for individual solidlike and liquidlike phases, "nonwetted" clusters (made of a solid and a liquid part on top of each other) were discovered.

Opposite of homogeneous clusters, alkali halides are bound through long-range attractive and *repulsive* forces. Any two ionic particles cannot swap as easily as in LJ clusters, for instance. Due to this added rigidity and also to the far lesser number of isomers at a given size, the disordered, liquidlike state appears very different, much stiffer in ionic clusters than in van der Waals clusters.[26] Precisely, the distinction between isomerization and liquidlike phase is not clear in alkali halides, whereas it is evident as soon as the size reaches approximately 7 in LJ clusters. The hierarchical character of the potential energy surface (PES) is then assumed to play a central role in the phases and phase changes.[28]

Various tools have been proposed to make the connection between the local structure of the configuration space and the thermodynamics of a cluster. First, the periodic quenching method of Stillinger and Weber[29] has been successfully applied to LJ clusters of various sizes[3] and also to other systems[31,32] including alkali halides.[25] This method allows a partitionning of the configuration space into various regions, each pertaining to a well-defined isomer. The samples of minima obtained by this method can further be used to build the thermodynamical functions of the cluster using the harmonic superposition

S1089-5647(98)00118-7 CCC: $15.00
Published on Web 02/20/1998

approximation of Wales.[7,18] Second, it has been shown by Wales and Berry[33] that the local curvature of the PES could be related to the Kolmogorov (K) entropy (see also refs 34, 35). The K entropy and the related Liapunov exponents measure the exponential rates of divergence or convergence of neighboring trajectories in the phase space. They are a measure of the "chaoticness" of the system, so that these quantities are interesting not only in the study of the local topography of the PES but also in the determination of the degree of disorder associated with the system motion.

Actually, since the first investigation in the LJ_3 cluster by Beck et al.,[36] these quantities have been shown in some cases to exhibit strong variations when isomerization[6,37,38] or melting[39−41] occurs. However, this is not a general behavior, since some species (LJ_7 or LJ_{17}) seem to have regular and smooth monotonic variations.[6,41]

For larger systems, some studies have pointed out the different behaviors of either the maximal Liapunov exponent (MLE)[41−44] or the entire Liapunov spectrum[45] in both ordered and disordered phases. Investigating the 7-, 13-, and 55-particle LJ clusters, Nayak and co-workers have concluded that the opening of the phase space was responsible for the significant increase of the MLE observed at the onset of melting.[39] These authors also studied heterogeneous 13-particle rare gas clusters and showed quite different variations of the MLE from that in homogeneous LJ_{13}.[40] More recently, they also showed differences between the phase space dynamics in magic LJ_{19} and nonmagic LJ_{17} clusters, as seen in the MLE behavior.[41] However, as recently shown by Kwon and Park,[44] the variations of the MLE at the solid−liquid transition seem to be continuous due to relaxation phenomena, even in periodic systems. Indeed this could also occur in LJ clusters inside the coexistence range.[46]

The present paper deals with phases and phase changes in small sodium fluoride clusters. Our main goal is to get further understanding of the relationship between structural isomerization, melting, and phase transitions. We specifically focus on three neutral clusters, $(NaF)_6$, $(NaF)_7$, and $(NaF)_{13}$. These systems are shown to exhibit both isomerization and melting phenomena at successive temperatures or energies. From Monte Carlo (MC) and MD simulations, we calculate caloric curves. Regular quenches along MC trajectories are performed in order to determine the various structures explored by the cluster in a given phase. MD simulations are also used to estimate the MLE. Its behavior is compared to that of other thermodynamical or geometrical quantities and to the behavior of the MLE in other systems.

We briefly describe in the next section the methods used in this work. Section III presents our results on $(NaF)_n$ with $n =$ 6, 7, and 13. We also relate these results with the previously studied $n = 4$ size, with a special emphasis on the Liapunov exponents, which we calculated. We discuss these results in section IV and conclude in section V.

II. Method

Classical Monte Carlo and isoergic molecular dynamics are carried out with the rigid core interaction potential $V(\{r_{ij}\})$, including a Born−Mayer (BM) repulsive term:

$$V(\{r_{ij}\}) = \sum_{i<j} \frac{q_i q_j}{r_{ij}} + A_{ij} \exp\left(-\frac{r_{ij}}{\rho}\right) \qquad (1)$$

where r_{ij} is the distance between ions i and j, q_i and q_j being their respective electric charge. A_{ij} and ρ are numerical parameters which define the repulsive BM potential representing the effects of Pauli exclusion forces. Their values are given by ab initio calculations:[47] $A_{++} = A_{--} = A_{+-} = 1138.82$ eV and $\rho = 0.517\,745$ Bohr. The use of more complicated model potentials, particularly those including multipole terms, is not justified in this work since we are only interested in thermodynamical, hence statistical, data. The extra computational effort added with these terms would have produced only minor differences.[25]

To prevent evaporation at high energies or temperatures, we enclose the cluster in a repulsive spherical potential, beginning at a radius R_0, which is twice the size of the ground structure. In both MC and MD simulations, it is defined by adding the following extra term to the potential energy:

$$V_{\mathrm{rep}}(\{\mathbf{r}_i\}) = \sum_i \chi[||\mathbf{r}_i|| - R_0]^4 H(||\mathbf{r}_i|| - R_0)/4 \qquad (2)$$

with $\mathbf{r}_i$ the position of ion i with respect to the cluster center of mass, and H the Heaviside step function, $H(x) = 0$ if $x < 0$ and $H(x) = 1$ if $x \geq 0$. χ is a numerical constant taken in practice as 100 atomic units.

The MC simulations are analyzed with the multiple histogram (MH) method.[48] This method provides accurate microcanonical density of states functions extracted from either canonical isothermal MC or MD simulations[8,14,49,50] or microcanonical isoergic MD simulations.[51,52] The density of states, in turn, provides canonical functions such as the internal energy, or its derivative, the heat capacity C_V:

$$C_V(T) = \frac{1}{k_B T^2}(\langle E^2\rangle - \langle E\rangle^2) \qquad (3)$$

where $\langle E\rangle$ denotes the canonical average of the total energy at temperature T.

The steepest descent quenching method[29] is used to quickly find and locate the minima on the PES along MC (or MD) trajectories. This method momentarily stops the simulation and solves the differential equations $\mathrm{d}q_i/\mathrm{d}\tau = -\partial V/\partial q_i$, where $\{q_i\}$ are the Cartesian coordinates, for $\tau \rightarrow \infty$ until a minimum is found within a typical uncertainty ϵ. It is particularly useful for studying the relationship between the potential surface and the thermodynamical behavior. For better precision, this search is ended with a conjugate gradient[53] local optimization. The percentages of quenched isomers are recorded as a function of the temperature, especially for $(NaF)_7$.

The isomer frequency table of Amar and Berry[49] is generalized to study the connectivity between several parts of the configuration space and also the possible coexistence phenomena. The data collected during regular quenches in a simulation are used to compute a matrix (q_{ij}) with q_{ij} the number of times an isomerization event occurs from isomer i toward isomer j. In the present case of ionic clusters, as we shall see below, one can define several "classes" of isomers which gather together some isomers close in energy and/or in geometry. Similarly, for a cluster with n classes of isomers, we define a $n \times n$ connectivity matrix (q_{ij}) with q_{ij} the number of times the cluster is found initially in class i and then in class j for the successive quenches. A difference from the original method of Amar and Berry is that we can also estimate the time spent in a single class. Of course, when T is low and the cluster remains in its ground geometry, only the first diagonal element is nonzero.

We have also implemented the eigenvector-following technique of Cerjan and Miller[55] improved by Wales,[56] for locating saddle points on the PES. This procedure was not used extensively, but only to calculate some energy barriers between isomers.

Various algorithms were used to calculate the geometries of $(NaF)_n$ clusters. In their respective ground states, $(NaF)_6$ is a double hexagon, $(NaF)_7$ is made of two cube corners placed front to front, and $(NaF)_{13}$ is the $3 \times 3 \times 3$ cube with a missing anion in the center of a face. MC simulations are performed at constant temperature using the standard Metropolis algorithm. The Verlet algorithm propagates Hamilton's equations of motion during MD runs at fixed total energy and zero angular momentum. A time step of 2×10^{-2} au keeps the energy to a constant value within 0.01% for simulations up to 10^6 time steps.

The rms bond length fluctuations δ is estimated along MC and MD trajectories. It is a very important quantity for measuring the rigidity degree of the cluster, at a given energy or temperature. Lindemann's criterion states that a phase change to a fluid state occurs as soon as δ reaches the value 0.1.

From the microcanonical MD simulations, we also calculate the largest Liapunov exponent λ. For a molecular system of size N with a $6N$-dimensional phase space Γ, $6N$ scalars $\{\lambda_i\}$ called Liapunov exponents can be defined as (in base e):

$$\{e^{\lambda_1}, ..., e^{\lambda_{6N}}\} = \lim_{m\to\infty} \{\text{Magnitude of eigenvalues of } \prod_{i=0}^{m-1} J_i\}^{1/m} \quad (4)$$

where $J_i = \partial F/\partial \mathbf{x}$ is the Jacobian of the transformation $d\mathbf{x}/dt = F(\mathbf{x})$, with $\mathbf{x}$ a vector of Γ with $6N$ coordinates. m is the total number of time steps; J_i is the Jacobian at step i. In a Hamiltonian system, the Liapunov exponents go by positive and negative pairs, and up to $3N-7$ of them can be strictly positive.[57] The maximal Liapunov exponent (MLE) quantifies the exponential rate of divergence of two initially close phase space trajectories. If a metric $d(\mathbf{x})$ is defined on Γ, the MLE λ can be more easily calculated by

$$\lambda = \lim_{k\to\infty} \lim_{d(\mathbf{x}_0)\to 0} \frac{1}{k} \ln \frac{d(\mathbf{x}_k)}{d(\mathbf{x}_0)} \quad (5)$$

The tangent space method of Benettin et al.[58] is used in MD simulations to calculate the MLE at several energies, for runs of 10^6 time steps equilibrated during 3×10^5 time steps. Such durations appear necessary to achieve a good convergence of λ, particularly for the bigger cluster $(NaF)_{13}$, although δ seems to need only 10^5 steps to reach a nearly constant value. Such a problem was previously raised by Berry and co-workers.[6,59] However, despite this attention paid to the convergence problem, the final value of λ may remain uncertain due to the fluctuations in the structure and energy of the cluster, which are extremal in the phase transition or isomerization regions.

III. Results

The caloric curves for the clusters $(NaF)_n$ with $n = 4$, 6, 7, and 13 are presented in Figure 1. The heat capacity $C_V(T)$ calculated with the multiple histogram MC approach was checked to coincide with the results of our recent MD version of the histogram method.[51] We also plotted in the same figure the Lindemann index δ as a function of temperature.

We first briefly discuss the case of $(NaF)_4$, which has been studied by several authors in the past.[22,24,25] In Figure 1a, the bell-shape of C_V versus T is very close to that of small LJ clusters. Both flat regions, at low and high temperatures, are representative of stable thermodynamical phases, respectively solidlike and liquidlike. In the former state, only vibrations of the ions around their equilibrium positions are seen. The amplitude of these vibrations increases with temperature or internal energy. On the contrary the "liquidlike" state may be characterized by permanent fluctuations between different isomers,[25] the time spent as a particular isomer being comparable to the time required to cross a saddle on the PES. For this system, we define two classes of isomers in a very simple way: the first class is made of only the ground structure, and the second class is made of all the other isomers. We have performed regular quenches along MC simulations at several temperatures and computed the connectivity matrix, which is given in Table 1. When $T = 500$ K, the times spent in the solidlike state (class I) and in the liquidlike state (class II) are of the same magnitude. This is indicative of coexistence between both phases. At higher temperatures, only the liquidlike phase is stable, with very few occurrences of the ground geometry.

Therefore the heat capacity peak marks the coexistence between both phases, and the range of coexistence may roughly be estimated by the width of this peak. The sharp rise of δ from a rather small value (<0.1) to higher values, consistent with Lindemann's criterion, is thus also indicative of this rigid−fluid transition. Indeed, because of the low number of isomers in the fluid state, one should speak of an isomerization dynamics rather than of a true liquid state. We shall discuss these questions later.

At first sight, the thermodynamics of $(NaF)_6$ could be thought as identical to that of $(NaF)_4$. Here again, the bell-shaped caloric curve gives evidence for a phase change from solidlike to a much more disordered state, with a coexistence range centered near the transition temperature (about 900 K.) δ increases near 900 K, but after a significant increase near 300 K, which has no apparent counterpart on the caloric curve. By performing regular quenches along MC trajectories, one can easily understand the phenomenon involved here. We plotted in Figure 2 the potential energy of the quenched structures as a function of the MC pseudotime, for two temperatures. At $T = 300$ K (curve a), the cluster only fluctuates back and forth between two structures, its hexagonal ground state (with energy $E_g = -4.290$ eV/ion) and the rectangular first excited state ($E_e = -4.280$ eV/ion.) Both isomers are connected through a saddle point with energy $E_s = -4.225$ eV/ion. These data allow a rough estimate of the minimal temperature required for isomerization to occur. We simply say that this temperature is proportional to the potential energy necessary to cross the saddle point, via the equipartition theorem:

$$T_t \sim \frac{2}{3N-6} \frac{E_s - E_g}{k_B} \quad (6)$$

Such an estimation leads to $T_t \sim 100$ K, for the hexagon $\rightleftharpoons$ rectangle isomerization of $(NaF)_6$. A more precise evaluation could be made with the calculation of isomerization rates, using Rice−Ramsberger−Kassel (RRK) models for instance.[24,25] In Figure 2b, the quenches carried out at 1000 K display a much more complicated spectrum of isomers. In this truly melted state, the cluster is no longer confined in the hexagonal/rectangular shape and may reach in practice any of the excited structures.

The intermediate phase of $(NaF)_6$ (before complete melting) can be viewed as a "hot solid", even if the low saddle point is constantly crossed, since no permutation between any two ions ever happens. However, this solid is particularly soft. Actually the Lindemann index δ comes close to (and even surpasses) 0.1.

Coming to $(NaF)_7$, the calculated thermodynamical curve in Figure 1c is yet of a new kind with respect to the smaller sizes.

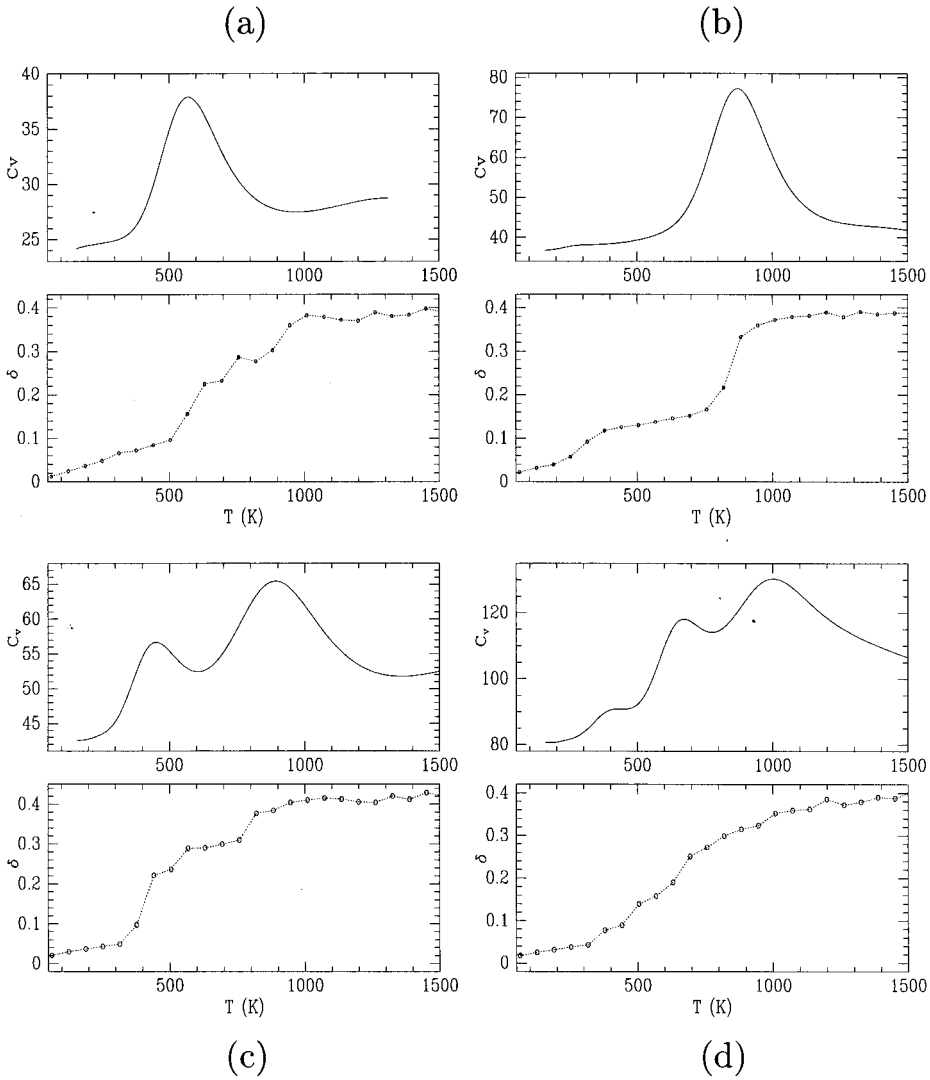

Figure 1. Canonical heat capacity $C_V(T)$ and root-mean-square bond length fluctuation $\delta(T)$. (a) $(NaF)_4$; (b) $(NaF)_6$; (c) $(NaF)_7$; and (d) $(NaF)_{13}$. C_V is given in units of k_B.

TABLE 1: Connectivity Matrix for $(NaF)_4$, for the Two Temperatures $T = 500$ K, $T = 700$ K[a]

$T = 500$ K		$T = 700$ K	
582	21	0	7
17	379	9	983

[a] The quenches are performed every 1000 cycles, for a total length of 10^6 MC cycles. The entry at row *i* and column *j* is the number of times the cluster was found in class *i*, and in the subsequent quench in class *j*.

The heat capacity exhibits two humps of similar heights and widths, the first centered near 450 K, the second near 900 K. Interestingly enough, the Lindemann index displays two separate increases at these temperatures, from solidlike to fluidlike, and then from fluidlike to another fluidlike, less stiff than the former. Here again, we have performed regular quenches in the course of the simulations. Several isomers found during these quenches are represented in Figure 3. Also, in Figure 4, we have represented the results of these quenches, for two temperatures, $T = 500$ K (curve a) and $T = 1000$ K (curve b.) This allows us to determine the underlying part of the PES actually explored by the cluster. Only a few isomers can be found at 500 K. In the range 500 K $\lesssim T \lesssim$ 900 K, no new excited state can be reached, although the time spent in any specific basin of the energy surface gets shorter as T grows. The collection of

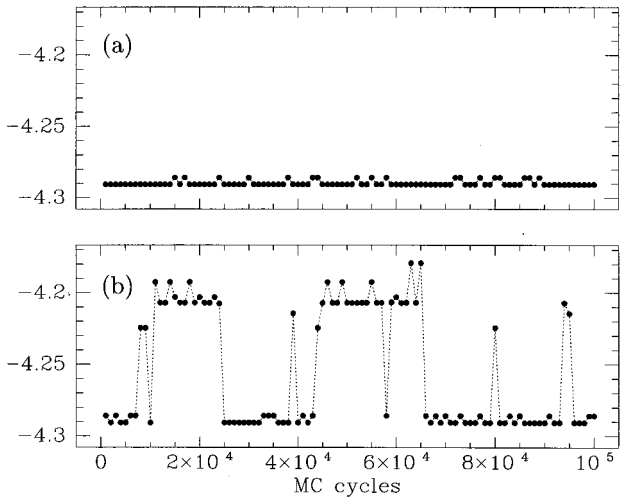

Figure 2. Energies of the isomers found by regular quenching of MC trajectories for $(NaF)_6$. The local minima are found by gradient optimization performed every 1000 cycles, for a total length of 10^5 cycles steps. (a) $T = 300$ K; (b) $T = 1000$ K. One MC cycle means two displacements for every atom in the cluster. The energy unit is in eV/ion.

isomers in this range has a remarkable common feature: all isomers are indeed made of either a capped double hexagon or

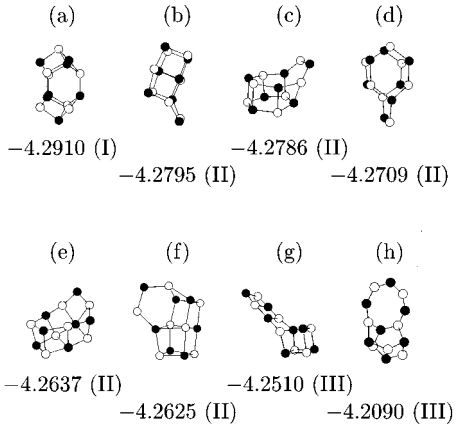

Figure 3. Some isomers of $(NaF)_7$, whose binding energies are given in eV/ion. The numbers I, II, and III refer to the classes described in the text.

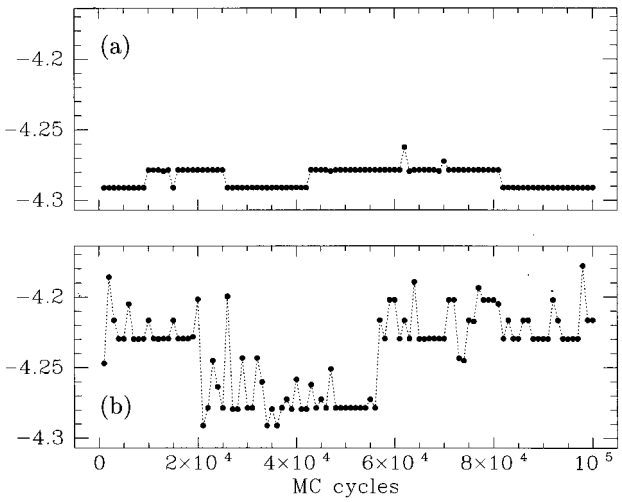

Figure 4. Two quenched MC trajectories for $(NaF)_7$. The quenches are performed every 1000 cycles, for a total length of 10^5 MC cycles. (a) $T = 500$ K; (b) $T = 1000$ K. The energy unit is in eV/ion.

a capped double cube (structures (b−f) in Figure 3.) Any isomer of this class can be written as $(NaF)_6 + NaF$, where $(NaF)_6$ is either in its hexagonal or its rectangular shape. We shall denote this class by the number II, class I being solely made of the ground state. Class III, at last, gathers together all the isomers not belonging to either class I or II (two of them are shown in Figure 3.)

The connectivity matrix was calculated at four temperatures and is given in Table 2. When $T = 450$ K, the cluster never reaches class III but isomerizes either from class I to class II or the reverse, or inside class II. It mainly stays in its ground geometry, but still coexists with the isomers of class II. When T is increased to 650 K, the times spent in either class I or class II change in the direction of class II, and the coexistence persists. At $T = 900$ K, the cluster is able to reach the highest isomers of class III, but is poorly found in the ground state. Moreover, the cluster leaves this stable geometry very easily, mostly toward class II. Here, classes II and III coexist. Finally, at $T = 1500$ K, the most stable state is the third class, with only few isomerizations to class II. These results show that the connection between classes I and III is made through class II.

We also recorded the percentages of finding the cluster, after quenching and independently of the previous quench, in class I, II, or III, as a function of temperature. The results are given

TABLE 2: Connectivity Matrix for $(NaF)_7$, for the Temperatures $T = 450$ K, $T = 650$ K, $T = 900$ K, and $T = 1500$ K[a]

$T = 450$ K			$T = 650$ K		
677	1	0	108	34	0
16	293	0	31	826	0
0	0	0	0	0	0
$T = 900$ K			$T = 1500$ K		
9	26	0	0	1	3
24	515	0	2	57	8
1	0	424	1	7	920

[a] The quenches are performed every 1000 cycles, for a total length of 10^6 MC cycles. The entry at row i and column j is the number of times the cluster was found initially in class i, and in the subsequent quench in class j.

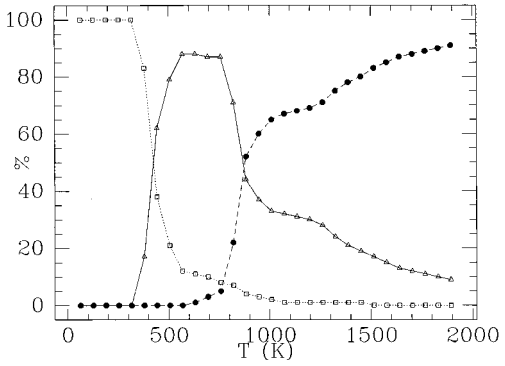

Figure 5. Percentage of isomers found along quenched MC trajectories versus the temperature, for the three classes of isomers: class I (□), class II (△), and class III (●).

in Figure 5. Both phase changes in the caloric curve appear exactly with the change of predominance of the classes.

Hence, we are led to a hierarchical partition of the potential surface of $(NaF)_7$. This is indeed plausible because the isomers of class II are all close in energy and in shape and well-separated from those in class III, either energetically or because they are of a very different shape. Actually, the minimal barrier height was found at −4.247 eV/ion, between structures a and f of Figure 3. This means that any saddle point between class II and class III is higher in energy (due to the variety of structures, such a saddle point could not be directly searched), confirming the existence of a high barrier between these classes. Equation 6 gives the estimate of 400 K for the temperature of first isomerization (transition class I ⇌ class II.) This is in agreement with the calculated C_V and δ curves. We thus think that the two phase transitions can be described as, respectively, (class I) ⇌ (class II) and (class II) ⇌ (class III.)

Contrary to $(NaF)_6$, the intermediate state of $(NaF)_7$ in the range 400 K $\lesssim T \lesssim$ 900 K can no longer be taken as a "hot solid". The quenches, and also δ, which exceeds over 0.2, unambiguously show that the state in this range is an isomeric liquid, rather similar to the liquidlike state of $(NaF)_n$ with $n \leq 6$, just above the onset of melting.[25] Now, the state above the second transition is of a different nature and comes closer to what one could identify as a true liquid state.

The case of $(NaF)_{13}$ is yet more complicated. The caloric curve in Figure 1d now exhibits two preliminary bends or humps (near 400 and 650 K) before the major peak at $T \sim 1000$ K. Each of these increases of internal energy with T is directly associated with corresponding increases of the Lindemann index $\delta(T)$. Three periodically quenched MC trajectories are shown in Figure 6. When temperature is low enough (<300 K), only the ground state consisting of a $3 \times 3 \times 3$ cube with an anion

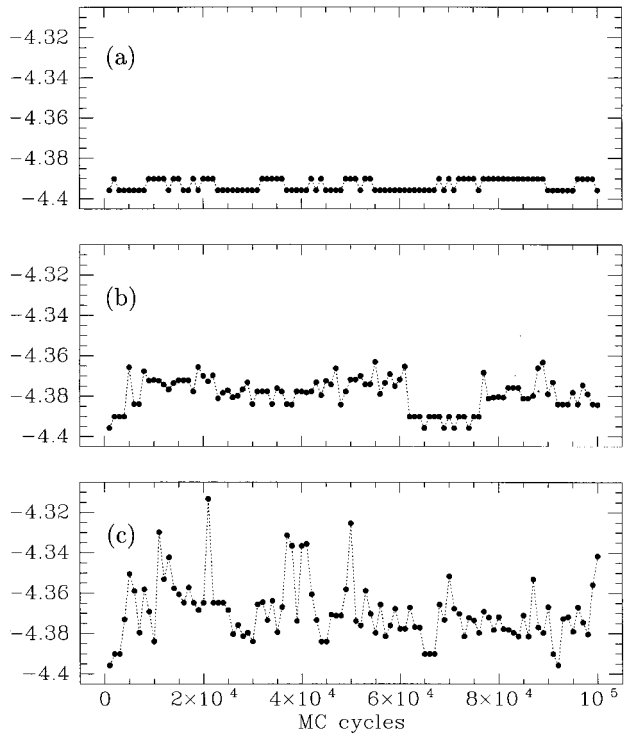

Figure 6. Three quenched MC trajectories for $(NaF)_{13}$. The quenches are performed every 1000 cycles, for a total length of 10^5 MC cycles. (a) $T = 500$ K; (b) $T = 700$ K; (c) $T = 1000$ K. The energy unit is in eV/ion.

missing in a face center (with energy −4.396 eV/ion) is found. The first excited isomer has the same structure except that the missing ion is now in a corner. Its energy is −4.389 eV/ion, and it is connected to the ground state through a saddle point with energy $E_s = -4.376$ eV/ion. Actually there are two similar isomers with cations instead of anions and vice versa, but these local minima are slightly higher in energy than the previous ones; furthermore they are not directly linked to the ground state on the PES. Therefore, unless the cluster is fully liquid, it cannot reach these isomers. Indeed, only two energies are seen in Figure 6a showing the distribution of quenched energies at $T = 500$ K. However, the picture is radically different from the "hot solid" in $(NaF)_6$, where two isomers were also observed in a temperature range. Here the isomerization corresponds to the move of a hole on the surface. When the temperature is high enough, the isomerization frequency increases and one has almost the picture of an embryonic surface melting, with the mobility of the missing anion becoming large. This is the reason the caloric curve shows a hump at the onset of this isomerization, while nothing is seen for $(NaF)_6$.

Before complete melting at about 1000 K, $(NaF)_{13}$ undergoes another transition, at 650 K. This transition leads from the previously described "moving hole" state to a more complex state consisting of numerous different noncubic isomers. From Figure 6b, the binding energies of these new isomers are in the approximate range [−4.385 eV/ion; −4.365 eV/ion]. A common feature of this new class of isomers is the compactness of their structures. This state could be called "compact fluid". On the contrary, the fluid state with T above 1000 K is more disordered, with structures partially made of chained ions Na^+ and F^-, loosely bound to the remaining, more compact part of the cluster. This new class of isomers may be characterized by higher configurational energies, going up to −4.315 eV/ion, as shown in Figure 6c.

We consider now the variations of the largest Liapunov exponent λ versus kinetic temperature T, represented in Figure 7. In the four cases $(NaF)_n$, $n = 4$, 6, 7, and 13, the logarithm of λ versus T displays the same behavior, that is, two linear parts with a changing slope. As concerns $(NaF)_4$, this change occurs at the same energy as the (single) increase of δ. This result is consistent with the picture of a clear signature of the phase transition on the MLE. However, contrarily to LJ clusters,[39] λ is continuous in the whole range of energies and does not exhibit strong variations at melting. Continuity in the variations of the MLE with temperature or internal energy (in the microcanonical ensemble) have also been observed in two- and three-dimensional periodic systems interacting through a repulsive soft-core potential.[44] In our case, more similarities can be found with the XY model of Butera and Caravati,[42] for which log λ displays, at the Kosterlitz-Thouless transition, variations very close to those observed in the present work. For the other clusters, the slope change occurs at the onset of isomerization. Above this point, the slope remains approximately constant, although several phase changes occur.

IV. Discussion

A major problem in studying phase transitions in clusters is the lack of a clear definition of what a solid or a liquid is in these species. In fact, if there is a general agreement to say that a phase transition occurs in the vicinity of a maximum of the caloric curve $C_V(T)$, with a phase coexistence range, it remains to characterize what these phases are. Of course a solid phase can be defined with no ambiguity, as the state where all particles vibrate only around their equilibrium positions. Actually, we could call "liquid" whatever is not solid, since the textbook definition of a liquid as something that takes the shape of the container is not applicable to small particles. A more precise definition, suggested by Rose and Berry,[25] relates the liquidlike character of a cluster to the general ease and velocity with which the system is able to move over the different permutational isomers of a single structure, inside a well of the potential surface or from well to well. With such a definition, some systems may exhibit original dynamical behaviors, neither solidlike nor liquidlike in some range of temperatures or energies.

As an example, the six-particle transition-metal cluster studied by Sawada and Sugano[31,32] undergoes a preliminary isomerization between the octahedric ground state and the first excited state, a distorded octahedron. This phase of perpetual isomerization was called a "fluctuating state" by these authors. This system is in a state very much like $(NaF)_6$ in its hexagonal $\rightleftharpoons$ rectangular isomerization process. Using the results of Rose and Berry for sizes $n = 4$ and 5,[25] we see that this equivalent of the fluctuating state occurs for sizes $n \leq 6$ in alkali halide microclusters. Furthermore, there is no significant maximum of the caloric curve at the onset of this state. For this reason and since it is just a kind of global breathing motion with no particle interchange, we propose to call this state a "hot solid."

However, for the larger clusters $(NaF)_7$ and $(NaF)_{13}$, the intermediate state exists over a wider range of temperature and, moreover, is separated from the solidlike phase by a phase transition. The complete melting occurs at a temperature T_m, and the definition of a liquid by Rose and Berry can be valid only for temperatures over T_m. And it is true that, rigorously, no permutation between cations or between anions of the ground state happen in the fluctuating state. But, since these intermediate phases are clearly separated from the solid one, as is visible in the caloric curves and in the Lindemann index, we suggest

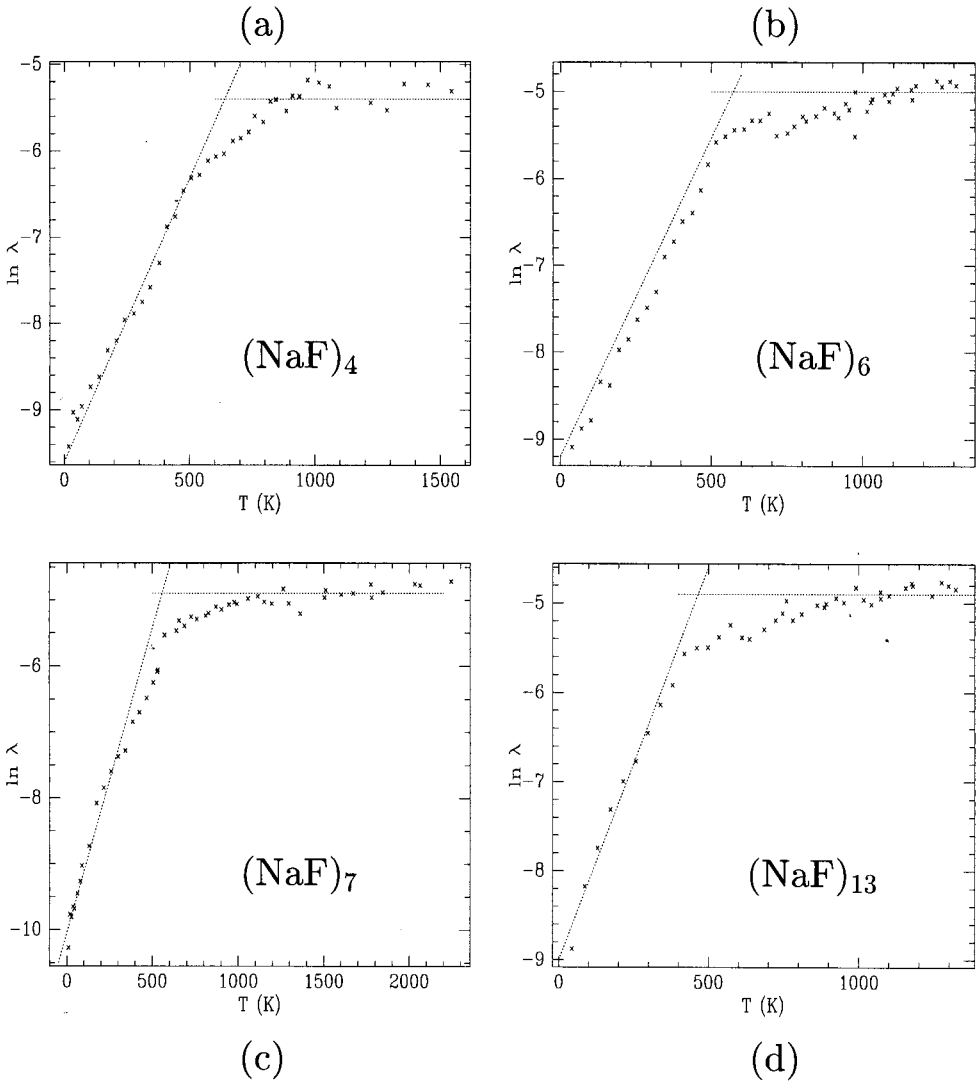

Figure 7. Maximal Liapunov exponent λ as a function of the kinetic temperature from MD simulations. (a) $(NaF)_4$; (b) $(NaF)_6$; (c) $(NaF)_7$; and (d) $(NaF)_{13}$. Units for λ are arbitrary.

differentiating these states from the previous "hot solid" and to refer to them as "isomerization fluids."

Now, we propose to call fluid isomerization transitions (FIT) the kind of transition involving an isomerization fluid state. When such a state occurs, at least two FITs are observed, one from solid to isomerization fluid and one from isomerization fluid to liquid. But more FITs can be observed, as in $(NaF)_{13}$, which shows three, the intermediate one relating two different isomerization fluid states. Often, the "true melting" toward a liquidlike state, where permutations within a single isomer occur, is hidden in the caloric curves by the preceding FIT. Indeed the FITs are thermodynamically well-defined events occurring with a sudden opening of the configuration space. The fluid isomerization states, as well as the "hot solids" such as $(NaF)_6$ between 300 and 800 K, can be directly associated with hierarchical levels in the PES. Each hierarchical level is associated with a certain class of stable structures, i.e., is the attraction basin of these structures. Two hierarchical levels are seen before that of complete melting for $(NaF)_7$, and three in the case of $(NaF)_{13}$. $(NaF)_6$ also has three levels, but the first two are close to each other. When the cluster undergo a FIT toward a higher level of the PES, it may still be found in the lowest levels. This coexistence phase phenomenon can be seen in a very clear way in the connectivity matrix computed in the present work for $(NaF)_7$. It is not obvious that this phenomenon could be seen in the probability distribution of the short-time averaged energies, since the gap in potential energies between classes is not especially large, in relation to what is observed in magic LJ clusters.[7] While it is revealed by the regular quenches, coexistence could also be investigated using the order parameter approach of Doye and Wales,[18] which generalizes the use of short-time averaged quantities to geometrical functions and their probability distributions. In some cases studied here, a good order parameter could be the index distance introduced by Sawada and Sugano,[31] in particular for the study of the hole diffusion in $(NaF)_{13}$. However, finding a suitable order parameter that could exhibit multimodal probability distribution in a coexistence phase is not a straightforward task in general. Larger magic, cubic sizes could better profit from this approach, for instance in studying the mechanisms of plane-by-plane melting and phase separation[19] or even nonwetting.[26]

The picture of a melting process occurring through successive FITs connecting more and more fully fluid states has no counterpart in bulk salts. One can thus expect the FITs and the melting to merge as size grows (see for instance the sharp transition of the magic size $K_{32}Cl_{32}$ investigated by Rose and Berry[26]). For nonmagic clusters, FITs might remain at larger sizes, and one can wonder what the characteristics of the corresponding phases are. The thermodynamical behavior of such systems could be rather close, in a way, to the bulk liquid−

liquid transitions observed for instance in sulfur. The FIT could then be viewed as a new kind of thermodynamical phase transition in clusters, besides the universal solid−liquid and the less common solid−solid[11] transitions.

As is apparent from above, the Lindemann index does not allow making a difference between an isomerization fluid and a true melted state. Another parameter has been suggested as representative of a phase transition,[39] which we want to turn to now: the largest Liapunov exponent as a function of the total energy in MD simulations. A detailed analysis of the relationship between the behavior of the K entropy with energy and the local properties of the PES was provided in a paper by Hinde and Berry.[34] In particular, the importance of the value of the negative curvature of the saddle point was emphasized: in LJ_3 for example, the low curvature of the linear saddle point allows the cluster to spend much of the time near the saddle once it can cross it, leading to the counterintuitive behavior of a decrease of the K entropy at the transition. For bigger LJ clusters such as LJ_7, or Morse clusters,[6,39] the MLE and the K entropy either do not change or change slope at the melting temperature, where the lowest saddle point can be crossed. This is indicative of high curvatures of the PES, the systems being unable to remain in the neighborhood of the saddle point for long times. From Figure 7 it appears that the MLE nearly reaches its highest value as soon as the cluster can isomerize and never drops at increasing energies. This means that, at this point, the cluster has reached its "maximum chaoticness." For $(NaF)_4$, this coincides with melting. $(NaF)_6$, on the other hand, becomes fully chaotic when the hexagonal $\rightleftharpoons$ rectangular process occurs; according to what has been said above, the cluster is a "hot solid" at this point. The further transformation to a true liquid has no effect on the variations of λ. In a similar way, $(NaF)_7$ and $(NaF)_{13}$ arrive at a maximal amount of chaos at the first FIT. It results from the analysis of Hinde and Berry[34] that (i) no negative curvature on the PES has an especially low value and/or (ii) the total number of degrees of freedom is much too large to allow for a momentary increase of harmonicity when crossing the lowest saddle points. Actually, this second effect has been invoked by Berry[35] to explain the smooth variation of the K entropy in LJ_7.

Once the lowest saddle points are crossed, the MLE shows no variation, although the cluster has access to larger parts of the PES for each thermodynamical change such as the FITs. Again, this is probably due to the large number of degrees of freedom, many of them not being involved in the melting process or the FITs.[35] It is nevertheless not yet obvious why the degree of chaos (measured here by the MLE) should reach a quasi constant value instead of increasing monotonically and regularly, as for LJ systems.[6,39,41] Is there an intrinsic "maximum chaoticness" for a small system, which would be reached immediately in our case and at much higher energies in van der Waals clusters? To our knowledge, this problem has never been raised before, at least in the cluster community. The largest Liapunov exponent appears to be unsensitive to the successive opening of the configurational space to new hierarchical regions, whereas a single isomerization process is sufficient to induce a global chaotic dynamics. Thus, considering these clusters just as dynamical systems, there is no difference between the "hot solid" of $(NaF)_6$ and the "isomerization fluid" of the larger clusters. Consequently, the information given by the MLE in thermodynamical simulations must be taken with some care, since the various phase changes may not necessarily be visible with variations of λ.

However, besides this apparent drawback, we see in the curve $\lambda(E)$ for $(NaF)_6$ a possible way to detect some low-temperature isomerization processes that have no thermal signature. The sensitivity of the MLE is even high enough to permit good estimations of the isomerization energies, while isomerization events are still rare.

V. Conclusion

In this work, we have investigated the thermodynamics and the chaotic dynamics of some small size-selected sodium fluoride clusters. The solid−liquid transition, which is usually a one-step process in rare gas clusters, becomes a multistep process made of several partial melting events. The cluster reaches various levels of increasing floppiness in the PES through "fluid isomerization transitions". Each of these levels is associated with a distinct class of isomers belonging to successive hierarchical parts of the configuration space. The partial transitions are characterized by an increase of the Lindemann index δ. They may be associated with an extra increase of the internal energy with temperature, when it leads to a fluid isomerization state. This situation occurs for $(NaF)_7$ and $(NaF)_{13}$. But they also may not display such variations, as it happens for $(NaF)_6$ in its state denoted as a "hot solid".

Our results address the problem of a general *thermodynamical* definition of the liquid phase in finite systems. Dynamical definitions[25] allow for a satisfactory understanding of the numerical liquid state seen in MD simulations. In particular, the "fluctuating state" of Sawada and Sugano,[31,32] similar to our fluid isomerization state, appears as an intermediate between the solid and the liquid. However, this definition does not permit distinguishing between the "hot solid" $(NaF)_6$ and the fluid isomerization states of $(NaF)_7$ and $(NaF)_{13}$, whereas the thermal effects are very different in both cases. We have supplemented the definition of Rose and Berry by taking into account these effects: the fluid isomerization transition occurs with a rise of the caloric curve, and events that do not have a thermal signature on this curve (even if δ abruptly increases) are not considered as part of the global melting. In our opinion, the description in terms of "fluid isomerization states" and "hot solids" is therefore more relevant to the multistage melting observed in ionic microclusters. Phase coexistence has clearly been observed between successive classes, during the fluid isomerization transitions, especially with the use of the isomer frequency matrix of Amar and Berry.[49] A possible complementary approach to the study of coexistence is the order parameter approach of Doye and Wales.[18]

We have also studied the variations with total energy of the largest Liapunov exponent λ. For any of the four clusters investigated here, λ exhibits strong variations, as $\log \lambda$ clearly changes slope at the onset of first isomerization. For $(NaF)_4$, this coincides with melting. For other clusters that isomerize before the true melting (either through simple processes for $(NaF)_6$ or through a FIT for larger sizes), no further variations are seen past the first isomerization, and the exponent remains at a nearly constant value. We have suggested that a possible reason for this constancy could be the large number of degrees of freedom, along with sharp saddle points leading to the higher levels in the configuration space. In this respect, ionic clusters share a common behavior with van der Waals clusters such as LJ_7.[6,35]

Some LJ clusters also display preliminary transitions in the phase space; LJ_{14}, for instance, may have its outer 14th atom capable of moving over the surface of the inner icosahedron in a range of energies.[18,60] There are no thermal effects, but a saddle

is effectively crossed. In the case of LJ_{29}, the surface more truly melts at energies lower than the melting energy, but again this occurs with very low thermal effects (contrarily to LJ_{34}).[15] We calculated the variations of λ in these systems, but surprisingly enough, absolutely no effect can be seen when the preliminary transition occurs.[61] Moreover, as shown by the present study, ionic clusters have nearly fully chaotic dynamics as soon as the lowest saddle point can be crossed on the PES, while LJ (and Morse) clusters do not seem to reach this kind of maximal "chaoticness" at melting. Thus it seems that there is no systematic link between an increase in the phase space open to the system and an increase in the "chaoticness" quantified by λ.

Actually, contrarily to other quantities such as δ, the maximal Liapunov exponent does not display universal variations with energy in clusters of atoms and molecules.[37−41,46] To summarize, the following behaviors have been observed: (i) λ may strongly grow at a transition (first transition in $(NaF)_n$, large magic LJ clusters, ...); (ii) λ may drop at the onset of some isomerization processes (small LJ and Morse clusters, ...); (iii) λ may not show any special variations, while other parameters give evidence for thermodynamical effects (LJ_7 and nonmagic LJ clusters, other transitions in $(NaF)_n$ ...); and (iv) depending on the model potential, λ may (NaF clusters) or may not (LJ and Morse clusters) reach a nearly maximal value at high energies.

Reasons for this nonuniversality are to be found in the topographic details of the potential surfaces, but general principles (apart from the number of degrees of freedom) are still lacking. Further information would be gained on this subject by investigating other model potentials and larger sizes.

Acknowledgment. We thank the reviewers for pointing out to us the work by Amar and Berry. Support by the CNRS, the Région Midi-Pyrénées, the Université Paul Sabatier, and the MESR is gratefully acknowledged. P.L. is especially grateful to the Institut Universitaire de France for providing financial support and good conditions for research.

References and Notes

(1) Briant, C. L.; Burton, J. T. *J. Chem. Phys.* **1975**, *63*, 2045.
(2) Kaelberer, J. B.; Etters, R. D. *J. Chem. Phys.* **1977**, *66*, 3233.
(3) Quirke, N.; Sheng, P. *Chem. Phys. Lett.* **1984**, *110*, 63. Jellinek, J.; Beck, T. L.; Berry, R. S. *J. Chem. Phys.* **1986**, *84*, 2783. Honeycutt, J. D.; Anderson, H. C. *J. Phys. Chem.* **1987**, *91*, 4950. Stillinger, F. H.; Stillinger, D. K. *J. Chem. Phys.* **1990**, *93*, 6013.
(4) Hoare, M. R. *Adv. Chem. Phys.* **1979**, *40*, 49. Braier, P. A.; Berry, R. S.; Wales, D. J. *J. Chem. Phys.* **1990**, *93*, 8745.
(5) Braier, P. A.; Berry, R. S.; Wales, D. J. *J. Chem. Phys.* **1990**, *93*, 8745.
(6) Hinde, R. J.; Berry, R. S.; Wales, D. J. *J. Chem. Phys.* **1992**, *96*, 1376.
(7) Wales, D. *J. Mol. Phys.* **1993**, *78*, 151.
(8) Labastie, P.; Whetten, R. L. *Phys. Rev. Lett.* **1990**, *65*, 1567.
(9) Wales, D. J.; Berry, R. S. *Phys. Rev. Lett.* **1994**, *73*, 2875.
(10) Boutin, A.; Rousseau, B.; Fuchs, A. H. *Europhys. Lett.* **1992**, *18*, 245.
(11) Boutin, A.; Maillet, J.-B.; Fuchs, A. H. *J. Chem. Phys.* **1993**, *99*, 9944.
(12) Maillet, J.-B.; Boutin, A.; Fuchs, A. H. *Phys. Rev. Lett.* **1996**, *76*, 4336.
(13) Bulgac, A.; Kusnezov, D. *Phys. Rev. B* **1992**, *45*, 1988.
(14) Poteau, R.; Spiegelmann, F.; Labastie, P. *Z. Phys. D* **1994**, *30*, 57.
(15) Calvo, F.; Labastie, P. *Chem. Phys. Lett.* **1996**, *258*, 233.
(16) Güvenç, Z. B.; Jellinek, J. *Z. Phys. D* **1993**, *26*, 304.
(17) Cheng, H.-P.; Berry, R. S. *Phys. Rev. A* **1992**, *45*, 7969.
(18) Doye, J. P. K.; Wales, D. J. *J. Chem. Phys.* **1995**, *102*, 9673.
(19) Wales, D. J.; Doye, J. P. K. *J. Chem. Phys.* **1995**, *103*, 3061.
(20) Kim, S. G.; Tománek, D. *Phys. Rev. Lett.* **1994**, *72*, 2418.
(21) Martin, T. P. *Phys. Rep.* **1983**, *95*, 169. Diefenback, J.; Martin, T. P. *J. Chem. Phys.* **1985**, *83*, 4585.
(22) Luo, J.; Landman, U.; Jortner, J. In *Physics and Chemistry of Small Clusters*; NATO ASI Series B; Jena, P., Rao, B. K., Khanna, S., Eds.; Plenum: New York, 1987; Vol. 158, p 155.
(23) Jortner, J.; Scharf, D.; Landman, U. In *Elemental and Molecular Clusters*; Benedek, G., Martin, T. P., Pacchioni, G., Eds.; Springer: Berlin, 1988; p 148.
(24) Heidenreich, A.; Schek, I.; Scharf, D.; Jortner, J. *Z. Phys. D* **1991**, *20*, 227.
(25) Rose, J. P.; Berry, R. S. *J. Chem. Phys.* **1992**, *96*, 517.
(26) Rose, J. P.; Berry, R. S. *J. Chem. Phys.* **1993**, *98*, 3246.
(27) Rose, J. P.; Berry, R. S. *J. Chem. Phys.* **1993**, *98*, 3262.
(28) Bixon, M.; Jortner, J. *J. Chem. Phys.* **1989**, *91*, 1631.
(29) Stillinger, F. H.; Weber, T. A. *Phys. Rev. A* **1982**, *25*, 978; *Phys. Rev. A* **1983**, *28*, 2408.
(30) Lynden-Bell, R. M.; Wales, D. J. *J. Chem. Phys.* **1994**, *101*, 1460.
(31) Sawada, S.; Sugano, S. *Z. Phys. D* **1989**, *12*, 189.
(32) Sawada, S.; Sugano, S. *Z. Phys. D* **1989**, *14*, 247.
(33) Wales, D. J.; Berry, R. S. *J. Phys. B* **1991**, *24*, L351.
(34) Hinde, R. J.; Berry, R. S. *J. Chem. Phys.* **1993**, *99*, 2942.
(35) Berry, R. S. *J. Phys. Chem.* **1994**, *98*, 6910.
(36) Beck, T. L.; Leitner, D. M.; Berry, R. S. *J. Chem. Phys.* **1988**, *89*, 1681.
(37) Morais, V. M. F.; Varandas, A. J. C. *J. Phys. Chem.* **1992**, *96*, 5704.
(38) Yurtsever, Y. *Europhys. Lett.* **1997**, *37*, 91.
(39) Nayak, S. K.; Ramaswamy, R.; Chakravarty, C. *Phys. Rev. E* **1995**, *51*, 3376.
(40) Nayak, S. K.; Ramaswamy, R. *J. Phys. Chem.* **1994**, *98*, 9260.
(41) Tanner, G. M.; Bhattacharya, A.; Nayak, S. K.; Mahanti, S. D. *Phys. Rev. E* **1997**, *55*, 322.
(42) Butera, P.; Caravati, G. *Phys. Rev. A* **1987**, *36*, 962.
(43) Bonasera, A.; Latora, V.; Rapisarda, A. *Phys. Rev. Lett.* **1995**, *75*, 3434.
(44) Kwon, K.-H.; Park, B.-Y. *J. Chem. Phys.* **1997**, *107*, 5171.
(45) Posch, H. A.; Hoover, W. G. *Phys. Rev. A* **1989**, *39*, 2175.
(46) Calvo, F. *J. Chem. Phys.*, in press.
(47) Giraud-Girard, J. Thèse de doctorat, Université Paul Sabatier, Toulouse, 1993.
(48) Ferrenberg, A. M.; Swendsen, R. H. *Phys. Rev. Lett.* **1989**, *63*, 1195. Bicharra, C.; Gaspard, J.-P.; Mathieu, J.-C. *Phys. Lett. A* **1987**, *119*, 462. Hammrich, O. *Z. Phys. B* **1993**, *92*, 501.
(49) Weerasinghe, S.; Amar, F. G. *J. Chem. Phys.* **1993**, *98*, 4967.
(50) Tsai, C. J.; Jordan, K. D. *J. Chem. Phys.* **1993**, *99*, 6957.
(51) Calvo, F.; Labastie, P. *Chem. Phys. Lett.* **1995**, *247*, 395.
(52) Fanourgakis, G. S.; Farantos, S. C.; Parneix, P.; Bréchignac, P. *J. Chem. Phys.* **1997**, *106*, 4954.
(53) Press: W. H.; Flannery, B. P.; Teukolsky, S. A.; Vetterling, W. T. *Numerical Recipes*; Cambridge University Press: Cambridge, 1986.
(54) Amar, F. G.; Berry, R. S. *J. Chem. Phys.* **1986**, *85*, 5943.
(55) Cerjan, C. J.; Miller, W. H. *J. Chem. Phys.* **1981**, *75*, 2800.
(56) Wales, D. J. *J. Chem. Phys.* **1989**, *91*, 7002. Wales, D. J. *J. Chem. Phys.* **1994**, *101*, 3750.
(57) Mayer, H. D. *J. Chem. Phys.* **1986**, *84*, 3147.
(58) Benettin, G.; Galgani, L.; Strelcyn, J. M. *Phys. Rev. A* **1976**, *14*, 2338.
(59) Amitrano, C.; Berry, R. S. *Phys. Rev. Lett.* **1992**, *68*, 729.
(60) Beck, T. L.; Jellinek, J.; Berry, R. S. *J. Chem. Phys.* **1987**, *87*, 545.
(61) Calvo, F.; Labastie, P. To be published.